# Measurement of the $E_R = 338$ keV resonance strength for $^{23}$Na$(p,\alpha)^{20}$Ne

C. Rowland, C. Iliadis, A. E. Champagne, and J. Mosher
*The University of North Carolina at Chapel Hill, Chapel Hill, North Carolina 27599-3255*
*and Triangle Universities Nuclear Laboratory, Durham, North Carolina 27708-0308*
(Received 31 January 2002; published 28 May 2002)

The absolute strength of the $E_R = 338$ keV resonance for $^{23}$Na$(p,\alpha)^{20}$Ne has been determined. The experiment was carried out by measuring the number of resonant $\alpha$ particles, integrated over the yield curve, simultaneously with the number of Rutherford scattered protons. The method applied in the present work is independent of target stoichiometry, uniformity, stopping power, beam straggling, and current integration. For the resonance strength, we obtained a value of $\omega\gamma = (7.16 \pm 0.29) \times 10^{-2}$ eV. Previous results are systematically higher, because the change of target stoichiometry under proton bombardment was not taken into account. With proper consideration, the present method can also be applied to other low-energy $(p,\alpha)$ resonances.

DOI: 10.1103/PhysRevC.65.064609 PACS number(s): 24.30.−v, 25.40.Cm, 25.40.Lw

## I. INTRODUCTION

The determination of absolute resonance strengths is important for a variety of topics in nuclear physics, particularly in nuclear astrophysics. Many important nuclear reactions in stars proceed through resonances and the thermonuclear reaction rates are directly proportional to the resonance strengths [1].

Most resonance strengths are derived from the step height of thick-target yield curves [2]. This method requires knowledge of the target stoichiometry, absolute stopping powers, absolute proton charge deposited on the target, and absolute detection efficiencies. All these factors are difficult to determine and are sources of potential systematic errors. Consequently, discrepancies by factors of 2 or more between different absolute resonant strength measurements are common in the literature. Relative measurements of resonance strengths are less difficult and literature values derived by different authors are usually in good agreement. Relative resonance strengths are frequently converted to absolute strengths by comparing the thick-target yield for the resonance of interest to the yield for a resonance of recommended standard strength.

In a previous paper [3], henceforth called ''paper I,'' we described a method of measuring absolute resonance strengths for $(p,\gamma)$ reactions which does not depend on the properties of the target (stoichiometry, stopping power, and uniformity) and the incident ion beam (current integration and beam straggling). Furthermore, reliable resonance strength standards for $(p,\alpha)$ reactions at low energies have not been reported in the literature. Therefore, in the present work we extend our previous method to the case of a $(p,\alpha)$ reaction. This method involves measuring the number of resonant $\alpha$ particles, integrated over the yield curve, simultaneously with the number of Rutherford-scattered protons.

We have chosen the $E_R = 338$ keV resonance[1] in the $^{23}$Na$(p,\alpha)^{20}$Ne reaction for our study, because this reaction is part of the Ne-Na cycle and is important for nucleosynthesis in various astrophysical sites, including globular cluster red giant stars [6] and novas [7].

The experimental equipment used in the present measurements is described in Sec. II, followed by the formalism of determining absolute resonance strengths for a $(p,\alpha)$ reaction in Sec. III. Our procedures for measuring resonance strengths and detection efficiencies are presented in Sec. IV. A summary is given in Sec. V. Throughout this work, $E_p$ and $E_R$ denote the proton bombarding energy and the resonance energy, respectively. All quantities are given in the laboratory system unless mentioned otherwise.

## II. EXPERIMENTAL EQUIPMENT

### A. Setup and targets

The present experiments were performed at the Triangle Universities Nuclear Laboratory (TUNL). The 200 kV minitandem accelerator [8] provided proton beams in the energy range $E_p \leqslant 480$ keV. The uncertainty in absolute energy and the energy spread were $\pm 2$ keV and 1 keV, respectively.

The experimental setup used for the resonance strength measurements is shown in Fig. 1. The proton beam entered the scattering chamber through a 3-mm-diam collimator, passed through the transmission target, and was stopped $\approx 1.5$ m away on a tantalum beam stop located outside of the chamber. Proton beam intensities on target were typically 80–300 nA. The scattering chamber with target ladder was electrically insulated from the beam line and the entrance collimator. Emission of secondary electrons was suppressed by using antiscattering slits and a permanent magnet, located behind and around the collimator, respectively. The scattering chamber together with the target ladder and beam stop acted as a Faraday cup for measuring the total current passing through the target.

A carbon backing foil of 20 $\mu$g/cm$^2$ thickness was floated on water and mounted on a stainless steel frame with a 1-cm-diam hole. NaCl was evaporated from a tantalum boat onto this foil under vacuum. The resulting target thickness was $\approx 5.0$ keV at proton beam energies of $E_p$

[1]Note that Ref. [4] quotes a value of $E_R = 338.6 \pm 0.6$ keV, whereas one obtains $E_R = 336.3 \pm 0.8$ keV from the quoted excitation energy [4] and the $(p,\gamma)$ $Q$ value [5].

 ©2002 The American Physical Society

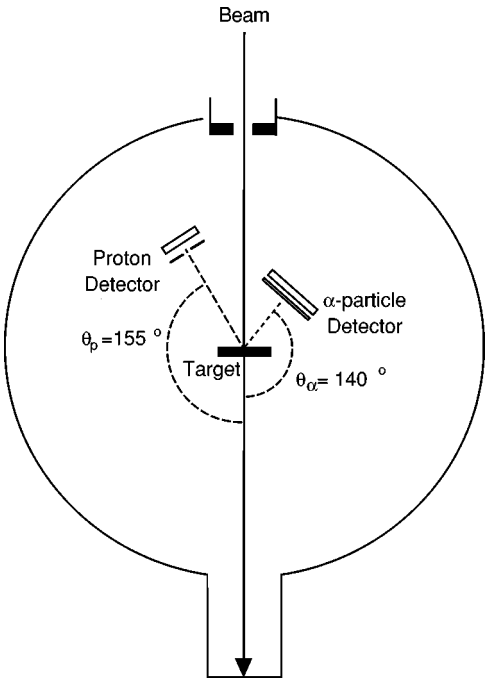


FIG. 1. Schematic diagram of the experimental setup used for the resonance strength measurement. Figure is not to scale.

≈340 keV. The NaCl target was tested frequently during the course of the experiment by monitoring the spectrum of backscattered protons. The target could withstand beam currents of up to 300 nA over several hours without noticeable deterioration in thickness or yield.

### B. Detectors

Elastically scattered protons were detected with a 100-$\mu$m-thick ion-implanted Si detector. A 0.8-mm-diam aperture was placed in front of the detector at a distance of 10.1 cm from the target. The energy calibration and resolution of the detector were obtained by measuring protons elastically scattered from a thin Au transmission target. The energy resolution was ≈10 keV. The detector angle was fixed at $\theta_p = 155°$ with respect to the beam direction, except for the angular distribution measurements.

The $\alpha$ particles were detected in a 1000-$\mu$m silicon surface-barrier detector with an active area of 450 mm$^2$. A 2.2-$\mu$m-thick Havar foil (CrCoNi alloy) was placed in front of the detector in order to prevent the large number of elastically scattered protons from reaching the counter. The detector was mounted at a distance of 4.2 cm from the target and the angle was fixed at $\theta_\alpha = 140°$ with respect to the beam direction.

Throughout the experiments, dead times and amplifier gain stabilities were monitored with a precision pulse generator.

## III. FORMULAS

The strength $\omega\gamma$ of a $(p,\alpha)$ resonance is defined by the expression [2]

$$\omega\gamma = \frac{2J+1}{(2j_p+1)(2j_t+1)}\frac{\Gamma_p\Gamma_\alpha}{\Gamma}, \tag{1}$$

with $J, j_p$, and $j_t$ the spin of the resonance state, projectile, and target nucleus, respectively. The partial widths $\Gamma_p$ and $\Gamma_\alpha$ describe the probability of formation and decay of the resonance through the proton and $\alpha$-particle channel, respectively.

The resonance strength $\omega\gamma$ is related to the area $A$ under a resonant yield curve [2],

$$\omega\gamma = \frac{2}{\lambda^2}\frac{1}{n_t}A, \tag{2}$$

where $\lambda$ is the de Broglie wavelength of the incident proton evaluated at the resonance energy and $n_t$ is the number of active target nuclei per unit area. It is shown in Ref. [2] that Eq. (2) is independent of straggling and beam homogeneity. In paper I we stated that Eq. (2) is applicable if the target thickness is much larger than the resonance width. However, closer inspection of the formalism described in Ref. [2] reveals that $\omega\gamma$ in Eq. (2) is independent of the resonance width as long as (i) the resonant cross section is described by the Breit-Wigner formula and (ii) the de Broglie wavelength and the partial widths are nearly constant over the width of the resonance. This consideration is important for the present work since the $E_R = 338$ keV resonance in $^{23}$Na$(p,\alpha)^{20}$Ne has a total width of ≈0.7 keV [4].

For sufficiently thin targets, the differential Rutherford cross section and the stopping power are approximately constant over the target thickness. Under this additional assumption it follows from the formalism presented in paper I that the $(p,\alpha)$ resonance strength $\omega\gamma_{p\alpha}$ may be written as

$$\omega\gamma_{p\alpha} = \frac{2}{\lambda^2}\frac{4\pi}{W_\alpha(\theta)}\frac{\Omega_p}{\Omega_\alpha}\int\frac{N_\alpha(E)}{N_{p'}(E)}\sigma_{Ruth}(E)dE, \tag{3}$$

where $N_{p'}$, $N_\alpha$, $\Omega_p$, and $\Omega_\alpha$ are the number of observed elastically scattered protons, the number of observed $\alpha$ particles, and the solid angles of the proton and $\alpha$-particle detectors (in steradian); $\sigma_{Ruth}$ is the differential Rutherford cross section; $W_\alpha(\theta)$ is the 0 angular distribution of the resonant $\alpha$ particles averaged over the solid angle of the $\alpha$-particle detector. All quantities in Eq. (3) are given in the center-of-mass system.

We emphasize that the resonance strength in Eq. (3) is independent of the properties of the target (stoichiometry, stopping power, and uniformity) and the beam (current integration and straggling), but depends on the observed numbers of resonant $\alpha$ particles and elastically scattered protons and on the angular distribution of the resonant $\alpha$ particles. Also note that $\omega\gamma_{p\alpha}$ depends on the ratio $\Omega_p/\Omega_\alpha$ and, consequently, is independent of the knowledge of *absolute* $\alpha$-particle and proton detection efficiencies. This ratio was measured directly in the present work with the $^{15}N(p,\alpha)^{12}$C reaction at $E_R = 340$ keV (Sec. IV B).

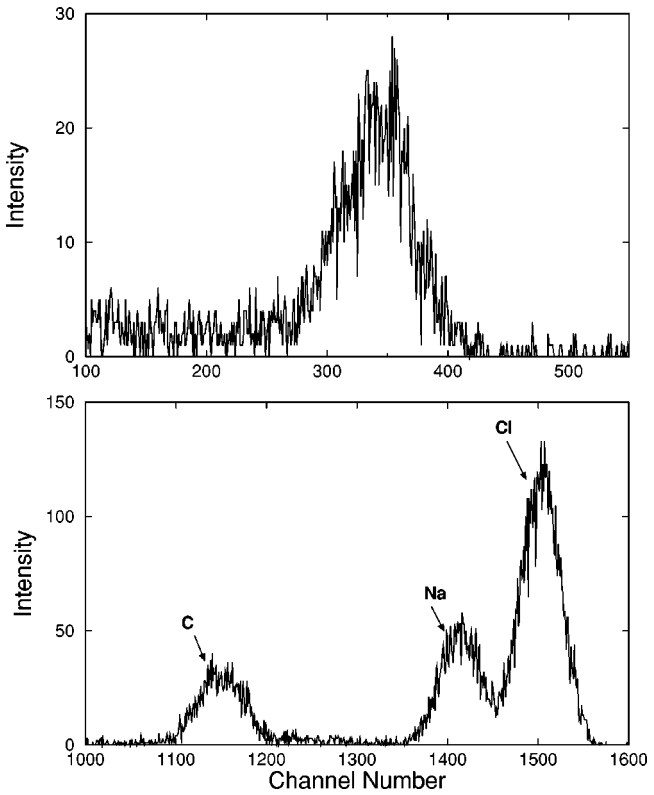


FIG. 2. Top: resonant $\alpha$-particle spectrum measured at $E_p = 341$ keV with the $\alpha$-particle detector located at $\theta_\alpha = 140°$. The peak centroid corresponds to an $\alpha$-particle energy of about 720 keV. Potential background from elastically scattered protons caused by pinholes in the Havar foil would occur below 300 keV (channel 130). Bottom: spectrum of elastically scattered protons measured with a NaCl transmission target, obtained at $E_p = 400$ keV and $\theta_p = 155°$.

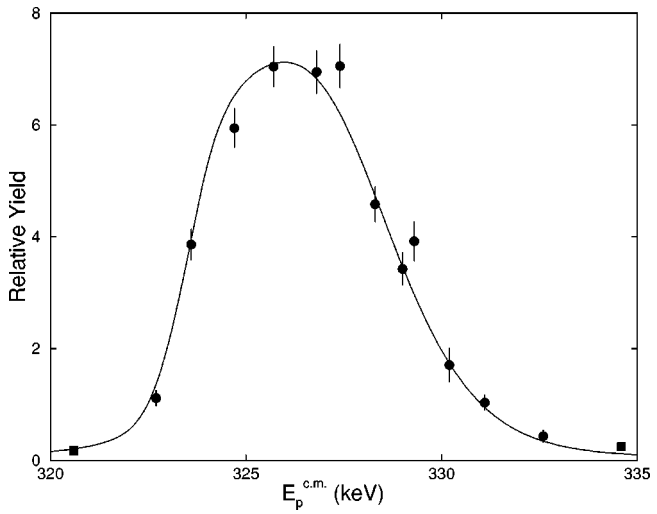


FIG. 3. Relative yield of $\alpha$ particles in the energy region of the 338 keV resonance in $^{23}$Na$(p,\alpha)^{20}$Ne. The solid line is a least-squares fit to the data (Sec. IV A). The squares represent upper limits.

## IV. PROCEDURE

### A. Yields of $\alpha$ particles and protons

A typical resonant $\alpha$-particle spectrum measured at $E_p = 341$ keV, with the $\alpha$-particle detector positioned at $\theta_\alpha = 140°$, is shown in the top part of Fig. 2. The $\alpha$-particle yield curve of the $E_R = 338$ keV resonance in $^{23}$Na$(p,\alpha)^{20}$Ne obtained with a 5-keV-thick NaCl transmission target is presented in Fig. 3. A least-squares fitting routine was used in order to determine the area under the resonant yield curve [3]. For the integral in Eq. (3) we obtain a value of $(42.70 \pm 0.87)$ fm$^2$ keV/sr.

A proton spectrum measured at $E_p = 400$ keV with the proton detector positioned at $\theta_p = 155°$ is displayed in the bottom part of Fig. 2. Contributions from Na and Cl and from the carbon backing are clearly resolved. It should be pointed out that the peak positions of protons elastically scattered by Na or Cl contain information regarding the bombarding energy and have been used in order to check the energy calibration of the accelerator.

Our method of measuring absolute resonance strengths depends on the assumption that the proton elastic scattering at low energies is well described by the Rutherford law. This assumption was verified in the present work by measuring the yield of scattered protons (i) as a function of bombarding energy at fixed detector angle (top left part of Fig. 4), and (ii) as a function of detector angle at constant bombarding energy (top right part of Fig. 4). The bottom part of Fig. 4 shows the yield curve for proton elastic scattering over the region of the $E_R = 338$ keV resonance in $^{23}$Na$(p,\alpha)^{20}$Ne. The data include on- and off-resonance runs. The solid lines represent the Rutherford yield normalized to the data points. No deviations from the Rutherford law were observed in any of the elastic scattering yield curves obtained in the present work.

### B. Detection efficiencies

The resonance strength $\omega\gamma_{p\alpha}$ given in Eq. (3) depends on the ratio of proton and $\alpha$-particle detection efficiencies. In the present work, the ratio was measured near the broad $E_R = 335$ keV$(J^\pi = 1^-)$ resonance in $^{15}$N$(p,\alpha)^{12}$C. It is shown in Ref. [9] that the angular distribution of the $^{15}$N$(p,\alpha)^{12}$C reaction is isotropic at $E_p = 340$ keV. Therefore the solid angle ratio $\Omega_p/\Omega_\alpha$ is given, apart from center-of-mass corrections, by the ratio of the observed $\alpha$-particle intensities in each detector. This measurement was performed with a thin $^{15}$N-enriched melamine target with the same setup as used for the resonance strength measurement. After correcting for the effects of finite target thickness and detector solid angle attenuation, we find for the ratio of proton and $\alpha$-particle detector solid angles a value[2] of $\Omega_p^{lab}/\Omega_\alpha^{lab} = (2.330$

[2]The quoted number has to be converted to the $^{23}$Na$+p$ center-of-mass system for use in Eq. (3). The result is $\Omega_p/\Omega_\alpha = (2.283 \pm 0.057) \times 10^{-4}$. Note that we are assuming a value of unity for the intrinsic efficiencies of the charged-particle counters for the detection of low-energy protons and $\alpha$ particles. This assumption has been verified in the present work by performing Monte Carlo simulations [14].

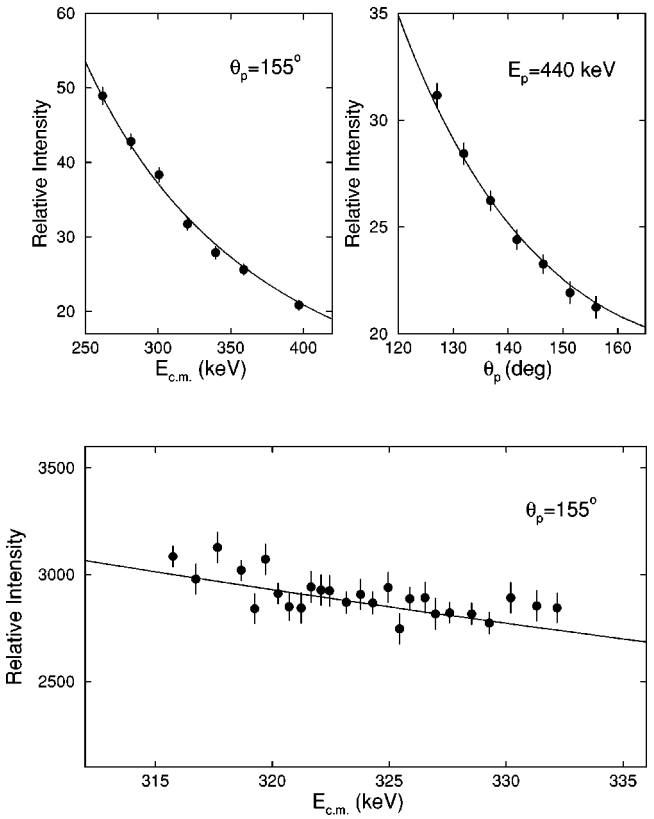


FIG. 4. Yields of elastically scattered protons from $^{23}$Na. The top left part of the figure shows the yield as a function of bombarding energy, with the proton detector located at $\theta_p = 155°$. The top right part shows the angular distribution obtained at $E_p = 440$ keV. The bottom part of the figure shows yields of elastically scattered protons over the region of the $E_R = 338$ keV resonance in $^{23}\mathrm{Na}(p,\alpha)^{20}\mathrm{Ne}$. The data include on- and off-resonance runs. In all diagrams the solid line represents the Rutherford yield normalized to the data.

$\pm 0.057) \times 10^{-4}$. This result has a much smaller error compared to the value $\Omega_p^{lab,abs}/\Omega_\alpha^{lab,abs} = (2.1 \pm 0.3) \times 10^{-4}$, which is calculated from the geometry of the charged-particle detectors.

### C. Angular distribution

As can be seen from Eq. (3), the resonance strength depends on the angular distribution of the resonant $\alpha$ particles. The angular distribution is given by [2]

$$W_\alpha(\theta_{\mathrm{c.m.}}) = 1 + \sum_k a_k Q_k P_k(\cos\theta_{\mathrm{c.m.}}), \tag{4}$$

where $a_k$, $Q_k$, and $P_k(\cos\theta_{\mathrm{c.m.}})$ are the angular distribution coefficients, solid angle attenuation coefficients, and Legendre polynomials, respectively. For the $E_R = 338$ keV($J^\pi = 1^-$) resonance in $^{23}\mathrm{Na}(p,\alpha)^{20}\mathrm{Ne}$, the angular distribution coefficients $a_k$ have been measured previously in Refs. [10,11]. The results of these independent measurements are in excellent agreement and a weighted average has been adopted in the present work. We have estimated the attenuation coefficients $Q_k$ according to the procedure given in Ref. [2]. The resulting value for the angular distribution, averaged over the solid angle of the $\alpha$-particle detector, is $W_\alpha(\theta_{\mathrm{c.m.}} = 141.2°) = 1.293 \pm 0.034$.

TABLE I. Absolute resonance strengths for the $E_R = 338$ keV resonance in $^{23}\mathrm{Na}(p,\alpha)^{20}\mathrm{Ne}$.

| $\omega\gamma \times 10^{-3}$ (eV) | | | | |
|---|---|---|---|---|
| Present | Ref. [12] | Ref. [10] [a,b] | Ref. [13] [a,c] | Ref. [11] [a] |
| $71.6 \pm 2.9$ | $97 \pm 19$ | $88 \pm 16$ | $72 \pm 18$ | $130 \pm 33$ |

[a]Obtained by using stopping powers from Ref. [14] (with an estimated error of 15%), assuming a target stoichiometry of Na:Cl = 1:1.

[b]Calculated from the reported differential $\alpha$-particle yield measured at $\theta_\alpha = 90°$.

[c]Calculated from the reported total $\alpha$-particle yield and corrected for angular distribution effects.

## V. RESULTS AND DISCUSSION

We obtain a value of $\omega\gamma_{p\alpha} = (7.16 \pm 0.29) \times 10^{-2}$ eV for the $E_R = 338$ keV resonance in $^{23}\mathrm{Na}(p,\alpha)^{20}\mathrm{Ne}$. The experimental error of 4.1% is given by uncertainties in the area under the resonance curve (2.0%), the ratio of the proton and $\alpha$-particle detection efficiencies (2.5%), and the $\alpha$-particle angular distribution (2.6%).

Previous values for the resonance strength were determined using the step height of the thick-target yield curve $Y_\alpha$ according to

$$\omega\gamma = \frac{2\epsilon_{eff}}{\lambda^2} \frac{Y_\alpha}{\Omega_\alpha W_\alpha(\theta)}. \tag{5}$$

All measurements (present and previous) have used NaCl targets. In this case, the effective stopping power is given by

$$\epsilon_{eff} = \epsilon_{Na} + \frac{N_{Cl}}{N_{Na}} \epsilon_{Cl}, \tag{6}$$

where $\epsilon_{Na}$ and $\epsilon_{Cl}$ are the stopping powers of protons in Na and Cl, respectively, at the resonance energy; $N_{\mathrm{Cl}}$ and $N_{\mathrm{Na}}$ are the number of Cl and Na target atoms per unit area. All quantities in Eqs. (5) and (6) are given in the center-of-mass system.

In Refs. [11,12], resonance strengths were obtained by assuming a target stoichiometry of Na:Cl = 1:1. In Refs. [10,13], only resonant $\alpha$-particle yields are presented. We have converted those yields into resonance strengths by using the stopping power values of [14] and a stoichiometry of Na:Cl = 1:1. All $\omega\gamma_{p\alpha}$ values are listed in Table I and are shown in the top part of Fig. 5. It is apparent that (i) the error of the present $\omega\gamma_{p\alpha}$ value is much smaller compared to previous results and (ii) most $\omega\gamma_{p\alpha}$ values reported in the literature are systematically higher compared to our result.

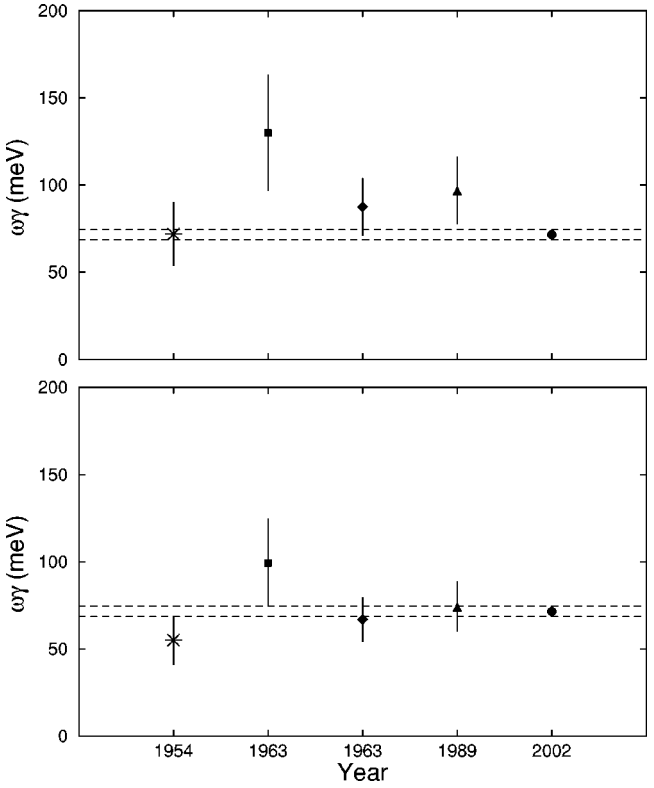


FIG. 5. Top: present value for the resonance strength compared with values reported in the literature, versus year of measurement. Symbols: star [13], square [11], diamond [10], triangle [12], and circle (present work). Bottom: present value for the resonance strength compared with literature results. The latter values have been corrected for a stoichiometry of Na:Cl=5:3 (see Sec. V). The dotted lines indicate the error of the present value.

We emphasize that a reliable resonance strength can only be obtained from Eqs. (5) and (6) if the target stoichiometry is accurately known. It is interesting to note that the stoichiometry of NaCl targets changes under proton bombardment. The effect is demonstrated in Fig. 4 of Ref. [15]. The NaCl targets lost significant amounts of chlorine during bombardment. After an accumulated charge of $\approx 8\times 10^{-5}$ C, the stoichiometry amounted to Na:Cl=5:3 and remained approximately constant for continued charge collection. An accumulated charge of $8\times 10^{-5}$ C is obtained after only 1.6 s with a 50-$\mu$A proton beam (as used in Ref. [12]) or after 260 s with a 300-nA proton beam (as used in the present work). Therefore, we conclude that the target stoichiometry of all NaCl targets used in measurements of the $^{23}$Na$(p,\alpha)^{20}$Ne reaction differs significantly from the commonly assumed value of Na:Cl=1:1. In the bottom part of Fig. 5 we show again all $\omega\gamma_{p\alpha}$ values, but now corrected for the variation in target stoichiometry (i.e., assuming a stoichiometry of Na:Cl=5:3). Clearly, the agreement between the present result (which is independent of target stoichiometry) and previous values has improved significantly.

## VI. SUMMARY AND CONCLUSIONS

The present work provides a standard resonance strength for the $^{23}$Na$(p,\alpha)^{20}$Ne reaction at $E_R = 338$ keV. The experiment was performed by measuring simultaneously the number of resonant $\alpha$ particles, integrated over the yield curve, and the number of Rutherford scattered protons. It has been shown that the method applied in this work is independent of the properties of the target (stoichiometry, stopping power, and uniformity) and the properties of the beam (current integration and straggling). Our result is $\omega\gamma_{p\alpha} = (7.16 \pm 0.29)\times 10^{-2}$ eV. The accuracy and precision of the resonance strength have been improved significantly compared to previous measurements. The influence of our result on the thermonuclear reaction rate of $^{23}$Na$(p,\alpha)^{20}$Ne will be investigated in a forthcoming paper [16].

Three necessary conditions have to be fulfilled for the application of the present method. First, the partial widths have to be approximately constant over the width of the resonance; i.e., the total resonance width should be less than several keV. Second, the Rutherford cross section and the stopping power have to be approximately constant over the thickness of the target; i.e., the target thickness should be less than $\approx 10$ keV. Third, the proton elastic scattering has to be well described by the Rutherford law.

## ACKNOWLEDGMENTS

The authors would like to express their gratitude to R. Fitzgerald, E. Harley, and R. Runkle for their help with this experiment and to B. Fisher for his assistance with the minimization algorithm. We also thank J. Görres for useful discussions. This work was supported in part by the U.S. Department of Energy under Contract No. DE-FG02-97ER41041.

[1] C. Rolfs and W.S. Rodney, *Cauldrons in the Cosmos* (University of Chicago Press, Chicago, 1988).
[2] H.E. Gove, in *Nuclear Reactions I*, edited by P. M. Endt and M. Demeur (North-Holland, New York, 1959).
[3] D.C. Powell, C. Iliadis, A.E. Champagne, S.E. Hale, V.Y. Hansper, R.A. Surman, and K.D. Veal, Nucl. Phys. **A644**, 263 (1998).
[4] P.M. Endt, Nucl. Phys. **A521**, 1 (1990).
[5] G. Audi and A.H. Wapstra, Nucl. Phys. **A595**, 409 (1995).
[6] R.M. Cavallo, A.V. Sweigart, and R.A. Bell, Astrophys. J. **492**, 575 (1998).
[7] C. Iliadis, A.E. Champagne, J. Jose, S. Starrfield, and P. Tupper, Astrophys. J. Suppl. Ser. (to be published).
[8] T.C. Black, B.E. Hendrix, E.R. Crosson, K.A. Fletcher, H.J. Karwowski, and E.J. Ludwig, Nucl. Instrum. Methods Phys. Res. A **333**, 239 (1993).
[9] A. Redder, H.W. Becker, H. Lorenz-Wirzba, C. Rolfs, P. Schmalbrock, and H.P. Trautvetter, Z. Phys. A **305**, 325 (1982).
[10] T.R. Fisher and W. Whaling, Phys. Rev. **131**, 1723 (1963).
[11] J. Kuperus, P.W.M. Glaudemans, and P.M. Endt, Physica (Am-

sterdam) **29**, 1281 (1963).
[12] J. Görres, M. Wiescher, and C. Rolfs, Astrophys. J. **343**, 365 (1989).
[13] F.C. Flack, J.G. Rutherglen, and P.J. Grant, Proc. Phys. Soc. London, Sect. A **67**, 68 (1954).
[14] J. P. Biersack and J.F. Ziegler, computer code TRIM, version 95.06, IBM Research, New York, 1995.
[15] B.M. Paine, S.R. Kennett, and D.G. Sargood, Phys. Rev. C **17**, 1550 (1978).
[16] C. Rowland *et al.* (unpublished).